Molecular Therapy
Methods & Clinical Development
Original Article

Preclinical evaluation of NG101, a potential AAV gene therapy for wet age-related macular degeneration

Juwon Shim,[1] Youyoung Kim,[1] Jeongyun Bak,[1] Sunhwa Shin,[1] Kyungwon Lee,[1] Yoon Hyung Hwang,[1] Hoon Young Kong,[1] and Joo Seok Han[1]

[1]Neuracle Genetics Inc., Seoul 02841, Republic of Korea

Age-related macular degeneration (AMD) is a leading cause of vision loss in individuals over the age of 55. Approximately 10%–15% of AMD patients develop choroidal neovascularization (CNV), leading to wet AMD (wAMD), which accounts for nearly 90% of AMD-related blindness. Inhibition of vascular endothelial growth factor (VEGF) is the standard treatment for wAMD. However, the frequent administration of the current treatment imposes a significant burden on wAMD patients. Therefore, there is an unmet need for treatments that require less-frequent administration. Here, we present findings on the safety and efficacy of NG101, a recombinant adeno-associated virus (rAAV) vector encoding aflibercept, an anti-VEGF agent, for wAMD therapy. A single subretinal injection of NG101 effectively reduced CNV lesion leakage and size at doses as low as 1×10^6 in mouse and 3×10^9 viral genomes per eye in cynomolgus monkeys. In cynomolgus monkeys, NG101-derived aflibercept expression in ocular tissues persisted for 1 year post-injection, indicating sustained therapeutic potential. Biodistribution analysis revealed that NG101 was primarily localized in ocular tissues. Only mild and transient ocular inflammatory responses were observed. Overall, these findings suggest that NG101, with its efficacy at low doses and sustained expression, is a promising therapeutic candidate for wAMD.

INTRODUCTION

Age-related macular degeneration (AMD) is the most common cause of vision loss in individuals over the age of 55 years, accounting for 6%–9% of legal blindness globally.[1] Approximately 10%–15% of AMD patients develop choroidal neovascularization (CNV), resulting in wet AMD (wAMD), which accounts for nearly 90% of AMD-related blindness.[2,3] The current standard treatment for wAMD is the intravitreal (IVT) administration of anti-vascular endothelial growth factor (VEGF) drug to impede new blood vessel growth and swelling.[4,5] However, this therapeutic regimen requires periodic IVT injections every 1–3 months, placing a substantial burden on patients, caregivers, and physicians.[6] Furthermore, periodic injections result in fluctuating peak and trough levels of VEGF during the intervals between dosing cycles.

To alleviate the burden and provide long-term expression of anti-VEGF agents, gene therapies for wAMD have emerged. Preclinical studies have been conducted on the efficacy and safety of gene therapies targeting VEGF *in vivo*,[2,7–10] and clinical trials are under way (these studies are registered at ClinicalTrials.gov: NCT05197270, NCT05536973, NCT04704921, and NCT05407636). Adeno-associated virus (AAV), found in various vertebrates including humans and non-human primates (NHPs), is devoid of pathogenicity in humans.[11] Thus, AAV is a leading platform for *in vivo* delivery of gene therapies. A recombinant AAV (rAAV) encapsidates vector genomes lacking any AAV protein-coding sequences instead contains therapeutic gene expression cassettes.[12] These vectors form episomal concatemers within the nucleus of host cells, providing long-term transgene expression.[13,14] Consequently, a one-time administration of gene therapy utilizing AAV vectors promises lifelong transgene expression. However, it is important to note that excessive doses of AAV to increase transgene expression can lead to toxicities. Clinical trials have shown dose-dependent adverse events.[15–17] Therefore, achieving precise delivery of minimal amounts of gene therapy products to the target site is crucial for ensuring safety.

The effective treatment of eye disease relies not only on the development of therapeutic agents but also on efficient delivery techniques to achieve optimal concentrations at the target tissue.[18] Therefore, the choice of the administration route for gene therapy products is pivotal. In ophthalmology, two injection routes prevail for gene therapies: IVT and subretinal (SR) injection.[19] IVT injection involves delivering AAV into the vitreous space, a procedure that can be easily performed in a doctor's office. However, the inner limiting membrane (ILM) acts as a barrier,[20] reducing the infection efficiency of AAV in the retinal region. This necessitates the use of higher doses, which increases the risk of unwanted immune responses. To address these limitations, new types of AAV, such as AAV.7m8 and R100, have been developed through capsid engineering to pass through the ILM and

Received 4 August 2024; accepted 29 October 2024;
https://doi.org/10.1016/j.omtm.2024.101366.

Correspondence: Joo Seok Han, Neuracle Genetics Inc., 145 Anam-ro, Seongbuk-gu, Seoul 02841, Republic of Korea.
E-mail: js.han@neuraclegen.com

infect the retina with significantly improved efficiency.[21,22] These advancements are undergoing clinical trials (these studies are registered at ClinicalTrials.gov: NCT05536973 and NCT05197270).

SR injection requires a surgical procedure for administration. Despite this, SR injection accurately delivers AAV to the target area, the outer retina, resulting in less leakage to other organs and a reduced immune response.[23] SR injection can effectively express therapeutic proteins in the required area with a relatively smaller dose, mitigating potential safety concerns associated with the AAV viral capsid. Two clinical trials are also using SR injection for wAMD (these studies are registered at ClinicalTrials.gov: NCT04704921 and NCT05407636).

NG101 is a recombinant, non-replicating AAV serotype 8 (rAAV8) expressing a coding sequence for aflibercept, a soluble recombinant protein composed of the binding domain 2 of VEGFR1 and domain 3 of VEGFR2, which is fused with the Fc region of human immunoglobulin G1 (IgG1).[24,25] Aflibercept binds VEGF-A, VEGF-B, and placental growth factor (PlGF), inhibiting the activation of VEGFR1 and human umbilical vein endothelial cell migration induced by PlGF.[26,27] Here, we elucidate the safety, efficacy, and durable gene expression of NG101. Aflibercept produced by NG101 effectively inhibited VEGF and exhibited binding specificity to VEGF-A and PlGF *in vitro*. A single SR injection of NG101 provided sustained aflibercept expression in NHPs. Moreover, NG101 significantly decreased CNV lesion leakage and size in mice and NHPs, comparable to the IVT injection of Eylea, at doses of 1×10^6 and 3×10^9 vg (viral genomes)/eye, respectively, without significant side effects. Collectively, based on our preclinical data, NG101 is a promising gene therapy candidate for wAMD.

RESULTS

Construction of NG101

NG101 is a recombinant, non-replicating AAV serotype 8 (rAAV8) expressing a coding sequence for aflibercept, a soluble protein composed of the binding domain 2 of VEGFR1 and domain 3 of VEGFR2, which is fused with the Fc region of human IgG1.[24,25] The aflibercept is expressed under a synthetic CAT311 promoter, which is composed of parts of the cytomegalovirus immediate-early enhancer/chicken β-actin (CAG) promoter and human elongation factor 1 alpha (EF-1α) intron. Following the promoter, the codon-optimized aflibercept gene is accompanied by multiple *cis*-elements, including the mutant woodchuck hepatitis virus posttranscriptional regulatory element (mWPRE), four copies of a target sequence to the microRNA 142-3p (miR142-3pTx4), and the bovine growth hormone polyadenylation sequence (bGH pA) (Figure 1A). These elements are flanked by two inverted terminal repeat (ITR) sequences designed to enhance transgene expression and reduce the immune response against the transgene product.[28,29]

CAT311 promoter-mediated robust and long-lasting ocular gene expression

The robustness and persistence of CAT311 promoter-mediated gene expression were examined using GFP as a reporter gene. Mice were SR injected with either vehicle, AAV8.CAGGFP (expressing GFP under CAG promoter), or AAV8.CAT311GFP (expressing GFP under CAT311 promoter). GFP signals were then measured by fundus photography (FP) images taken at various time points (Figure S1A). GFP signals in the eyes of mice administered AAV8.CAT311GFP were evident from 4 weeks post-injection, peaked at week 8, and persisted until week 51 (Figures S1B and S1C). Importantly, compared to the AAV8.CAGGFP group, the GFP signals in the AAV8.CAT311GFP group were significantly higher throughout the observation period. At 51 weeks post-injection, mice were sacrificed, and GFP levels were quantified by ELISA (Figure S1D). One year post-injection, the mean GFP level in the eyes of mice injected with AAV8.CAT311GFP was 185 ng/mg, compared to 55 ng/mg in the eyes of mice injected with AAV8.CAGGFP, indicating that the CAT311 promoter drove gene expression that was 3.4 times higher. Collectively, these data suggest that the CAT311 promoter enables robust and long-lasting transgene expression *in vivo*, outperforming the CAG promoter in terms of gene expression robustness in the eye, despite its significantly shorter length.

In vitro bioequivalence of aflibercept produced by NG101 and Eylea

We initially assessed the structural and functional integrity of NG101. The identity and purity of NG101 were examined by SDS-PAGE followed by SYPRO Ruby staining (Figure 1B). All three VP proteins, VP1–VP3, were detected at the anticipated ratio,[30] with little to no non-specific bands. Next, NG101-derived aflibercept was produced *in vitro* to evaluate its equivalence to Eylea. Seventy-two hours after transducing CHO-K1 cells with NG101, the culture medium was collected and analyzed alongside Eylea by immunoblotting (Figure 1C). Aflibercept produced by NG101 and Eylea showed similar sizes, with a molecular weight of approximately 115 kDa.[31]

In HEK293 cells, aflibercept expression was dose-dependent 48 h following transduction (Figure 1D). The biological activity of aflibercept from NG101 was evaluated using a VEGF bioassay with engineered HEK293 cells that express luciferase upon VEGF binding to VEGFR2. Aflibercept disrupts this interaction, resulting in reduced luciferase expression. Aflibercept from NG101 effectively inhibited VEGF, demonstrating equivalency to Eylea (Figure 1E). The half-maximal inhibitory concentration values were 33.62 ng/mL for NG101-derived aflibercept and 38.89 ng/mL for Eylea.

Ligand-binding selectivity was also assessed using an ELISA (Figures 1F–1H). The aflibercept from NG101 specifically bound to VEGF-A_{165} and PlGF, but not to hepatocyte growth factor (HGF), mirroring the binding profile of Eylea. The half-maximal effective concentration values for VEGF-A_{165} binding were 0.1038 nM for NG101-derived aflibercept and 0.1115 nM for Eylea, while for PlGF they were 0.9091 nM and 1.219 nM, respectively. Taken together, these findings demonstrate that aflibercept produced by NG101 is equivalent to Eylea in terms of VEGF binding and inhibition *in vitro*.

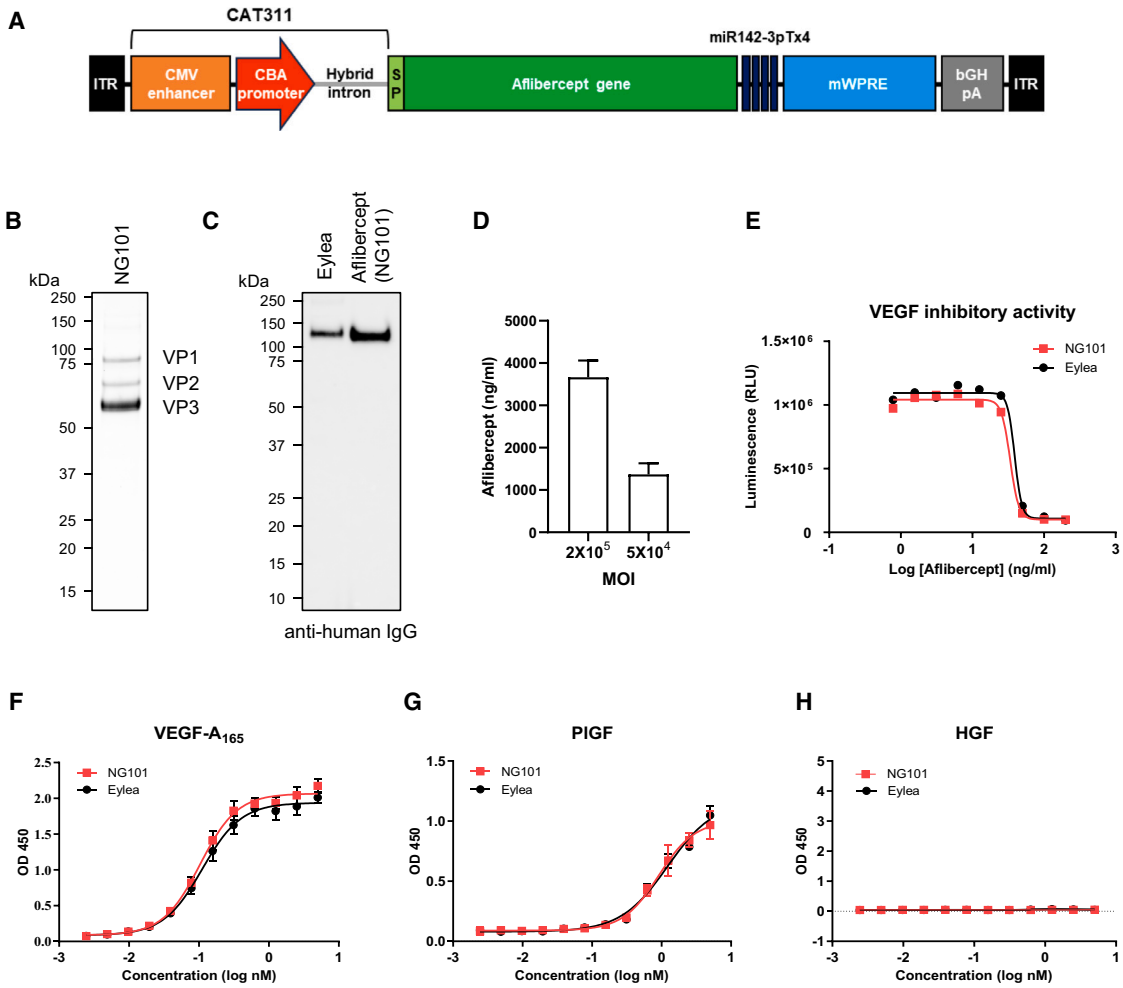

Figure 1. Aflibercept produced by NG101 binds to and inhibits VEGF signaling comparable to Eylea *in vitro*

(A) Graphical scheme of aflibercept expression cassette of NG101. (B) Purity of NG101 was assessed by SYPRO Ruby-stained SDS-PAGE (1×10^{10} vg/lane). (C) CHO-K1 cells were transduced with NG101 (MOI: 2×10^5). After 72 h, aflibercept produced by NG101 and Eylea were analyzed by non-reducing SDS-PAGE and immunoblotting. The Fc region of aflibercept was detected by an anti-human IgG antibody. (D) HEK293 cells were infected with NG101 at the indicated MOI. Forty-eight hours after infection, aflibercept levels in the culture medium were measured by ELISA. Data are shown as mean ± SD. (E) The VEGF inhibitory activities of aflibercept produced by NG101 and Eylea were evaluated. (F–H) The binding selectivity of aflibercept produced by NG101 and Eylea to recombinant VEGF-A_{165} (F), placental growth factor (PlGF) (G), and hepatocyte growth factor (HGF) (H) were evaluated. OD_{450}, optical density at absorbance 450 nm; RLU, relative luminescence unit.

Efficacy of NG101 in suppressing CNV in mice

To investigate the therapeutic potential of NG101, we examined whether its administration effectively induces aflibercept expression and consequently prevents laser-induced CNV formation in mice. Mice received SR injections of NG101 at doses ranging from 1×10^6 to 1×10^9 vg/eye 28 days prior to CNV induction, allowing sufficient time for the expression of NG101-derived aflibercept. In contrast, for the Eylea treatment group, Eylea was IVT injected at 40 μg/eye immediately after CNV induction. Ten days post-induction, we assessed CNV lesion leakage and size using fluorescein angiography (FA) and optical coherence tomography (OCT) (Figure 2A). Aflibercept expression in the whole-eye lysates occurred in a dose-dependent manner (Figure 2B), with all dose levels of NG101 resulting in aflibercept concentrations similar to or higher than those from IVT administered Eylea.

Ten days after CNV induction, fluorescent contrast agents were intraperitoneally injected into mice. The corrected total fluorescence (CTF) measured from FA images served to assess vascular leakage in CNV lesions. The size and density of CNV lesion leakages were significantly reduced in both the Eylea and NG101 (1×10^6 to 1×10^9 vg/eye) groups compared to the vehicle group. Notably, CTF levels were significantly lower in all NG101 groups than in the Eylea group (Figures 2C and 2D).

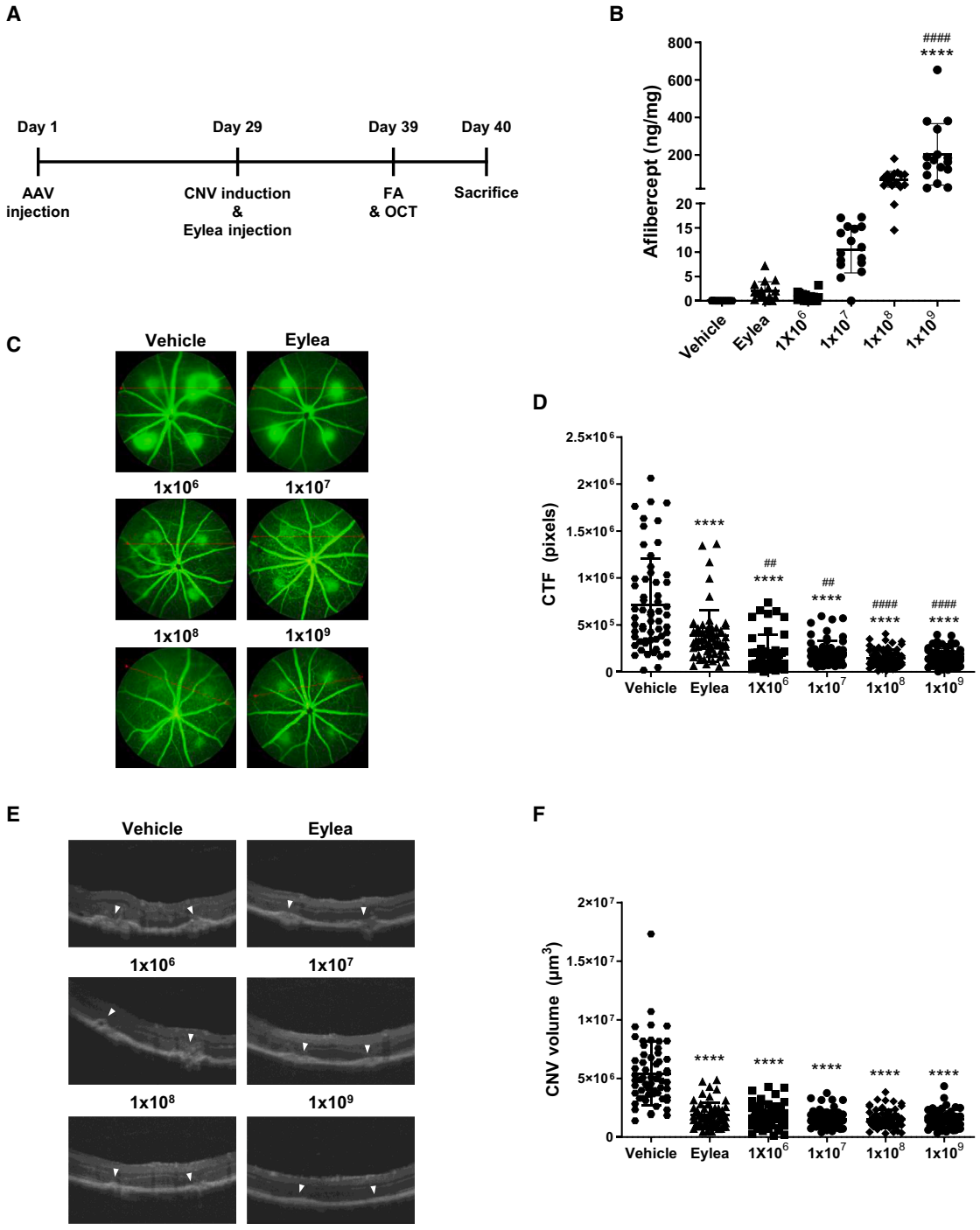

Figure 2. NG101 administration prevents laser-induced CNV formation in mice

Mice were administered either NG101 subretinally (SR) at the indicated doses (1×10^6 to 1×10^9 vg/eye) or vehicle (formulation buffer) 28 days prior to CNV induction, or with Eylea (40 µg/eye) intravitreally (IVT) once immediately after CNV induction. (A) Overview of efficacy testing in the mouse model of laser-induced CNV. (B) Aflibercept expression was measured 11 days after CNV induction by ELISA. Data are shown as mean ± SD. (C) Representative fluorescein angiography (FA) images are shown. (D) The CNV lesion leakage was evaluated. Data are shown as mean ± SD. (E) Representative OCT images are shown. Arrowheads indicate CNV lesions. (F) The volume of CNV lesions was measured. Data are shown as mean ± SD. (B, D, and F) Statistical analysis: one-way ANOVA. $^{****}p < 0.0001$ versus vehicle; $^{\#\#}p < 0.01$ and $^{\#\#\#\#}p < 0.0001$ versus Eylea.

Table 1. Animal group assignment

Test article	Dose level, vg/eye	Dose volume, μL/eye	Sex	Animal ID	Injection day	Laser treatment day	Sacrifice day
Vehicle	0	100	M	P0001	1	57	88
				P0002	1	57	88
				P0003	1	57	365
			F	P0401	1	57	86
				P0402	1	57	86
				P0403	1	57	365
Eylea	2 mg/eye	50	M	P0101	57	57	88
				P0102	57	57	88
				P0103	57	57	88
NG101	3×10^9	100	M	P0201	1	57	88
				P0202	1	57	88
				P0203	1	57	365
			F	P0501	1	57	86
				P0503	1	57	86
				P0504	1	57	365
NG101	6×10^9	100	M	P0301	1	57	88
				P0302	1	57	88
				P0303	1	57	365
			F	P0601	1	57	86
				P0602	1	57	86
				P0603	1	57	365

Concurrently, OCT was utilized to examine the CNV-induced retinal area, measuring the cross-sectional area of the CNV lesions either horizontally or vertically. The volume of CNV lesions, assessed by OCT, increased in the vehicle group but was suppressed in both the Eylea and all NG101 groups compared to the vehicle group (Figures 2E and 2F). However, no significant differences in the volume of CNV lesions were observed between the Eylea group and the NG101 groups. Collectively, these results demonstrate that even the lowest dose of NG101 significantly inhibits the growth of new blood vessels, showing efficacy that is statistically comparable to or superior to Eylea.

Aflibercept expression following SR administration of NG101 in NHPs

Following these results in mice, we extended our evaluation to the safety and efficacy profile of NG101 in NHPs. In the initial study, cynomolgus monkeys (1 male and 1 female per group) received SR injections of NG101 at doses ranging from 3×10^{10} to 1×10^{12} vg/eye. Eight weeks post-injection, aflibercept expression levels in ocular tissues were assessed (Figure S2). The retina exhibited the highest aflibercept levels in animals that received 3×10^{10}, 1×10^{11}, or 3×10^{11} vg/eye, while the highest concentrations in the vitreous humor (VH) occurred in animals given 1×10^{12} vg/eye (Figures S2A and S2C). The aqueous humor (AH) consistently showed the lowest aflibercept levels across all groups (Figure S2D). Previous studies with NHPs showed that an IVT injection of ADVM-022 at a dose of 2×10^{12} vg/eye nearly eliminated grade 4 CNV lesions, with retinal aflibercept concentrations of 3.5–7.3 μg/g at doses ranging from 2×10^{11} to 2×10^{12} vg/eye.[32,33] A phase 1 clinical study further confirmed that 2×10^{12} vg/eye is not the minimum effective dose.[34] These studies suggest that a retinal aflibercept concentration of 3–10 μg/g is expected to have a therapeutic effect on wAMD. Taking into account the strong correlation between aflibercept concentration and dosage and noting a retinal aflibercept concentration of 44 ng/mg after a single SR injection of NG101 at 3×10^{10} vg/eye (Figure S2A), we selected doses of 3×10^9 and 6×10^9 vg/eye for subsequent studies. These doses are aimed at achieving a retinal aflibercept concentration range of 3–10 μg/g tissue, expected to provide therapeutic efficacy in NHPs.

Efficacy of NG101 in laser-induced CNV model in NHPs

To further assess the efficacy and safety profile of NG101 in an NHP CNV model, an experiment was conducted where three male and three female cynomolgus monkeys were grouped and administered either a vehicle or NG101 at doses of 3×10^9 or 6×10^9 vg/eye via bilateral SR injection on day 1 (Table 1). Fifty-six days after NG101 administration (on day 57), laser-induced CNV was performed on all animals. In the Eylea group, three male cynomolgus monkeys received an IVT injection of Eylea at a dose of 2 mg/eye immediately following CNV induction. Approximately 3 months post-injection,

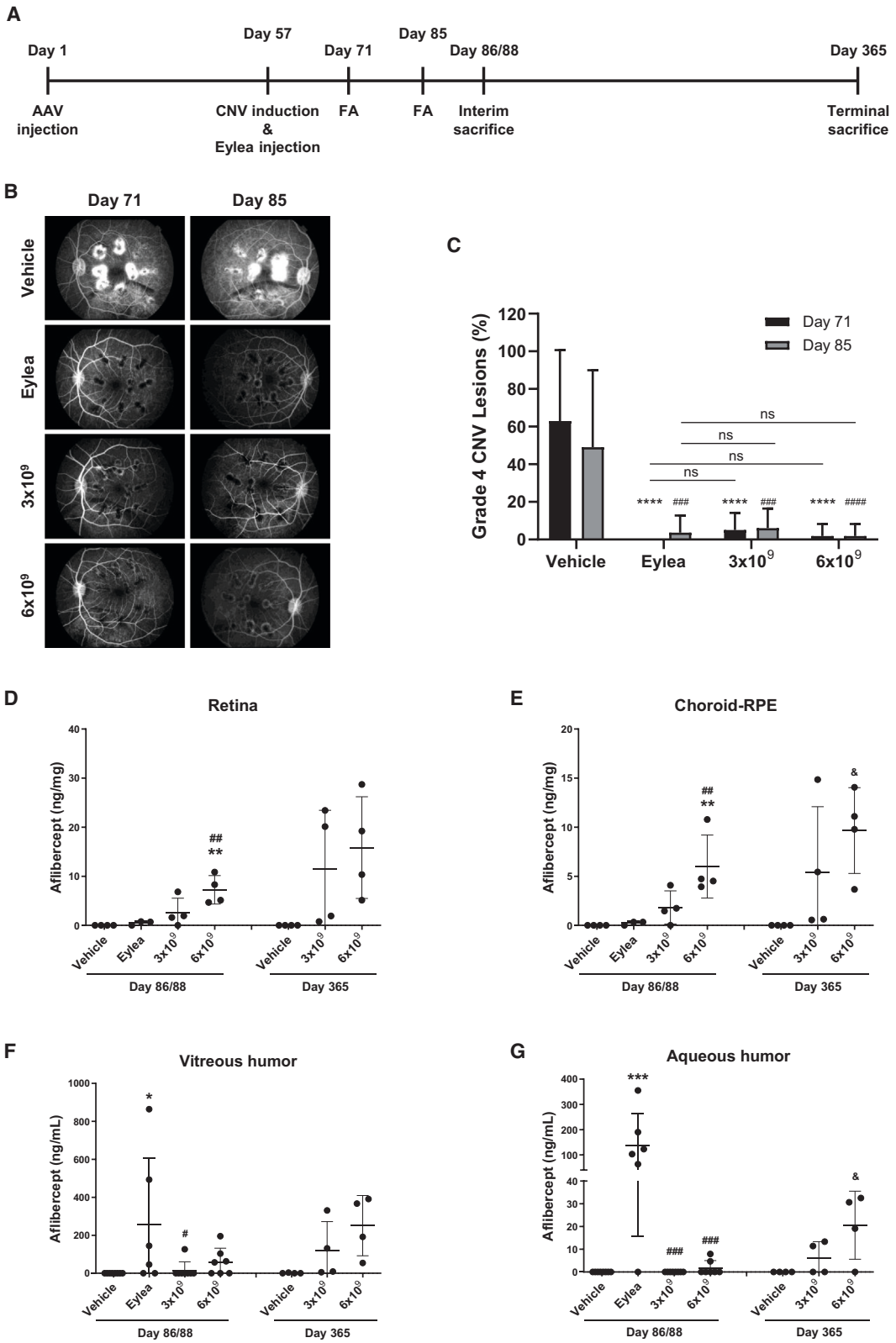

(legend on next page)

two males and two females from the vehicle and NG101 groups (3×10^9 or 6×10^9 vg/eye), along with all animals from the Eylea group, were sacrificed. The remaining animals were sacrificed on day 365 (Figure 3A). The incidence of clinically relevant grade 4 CNV lesions was determined using FA images.[35] On day 71, 2 weeks post-CNV induction, 63% of the eyes administered vehicle exhibited grade 4 CNV lesions, whereas none of the eyes treated with Eylea showed such lesions (Figures 3B and 3C). On day 85, 4 weeks post-CNV induction, the occurrence of grade 4 lesions was 49% in the vehicle group and 4% in the Eylea group. NG101 proved highly effective at preventing grade 4 CNV lesions on days 71 and 85 in animals administered either 3×10^9 vg/eye (5% and 6%, respectively) or 6×10^9 vg/eye (2% on both days), demonstrating efficacy comparable to Eylea.

NG101-mediated sustained expression of aflibercept in NHPs

To further evaluate transgene expression levels after a single SR injection of NG101, various ocular tissues including retina, choroid-retinal pigment epithelium (RPE), VH, and AH were analyzed. Aflibercept was detected in the ocular tissues of animals administered NG101 in a dose-dependent manner (Figures 3D–3G). Notably, due to the route of administration, aflibercept expression by NG101 was predominantly higher in the retina and choroid-RPE rather than VH and AH, whereas in the Eylea group, aflibercept concentrations were higher in VH and AH. Moreover, NG101 groups demonstrated sustained, and even elevated, ocular aflibercept levels up to day 365. These findings indicate that a single SR injection of NG101 at doses of 3×10^9 and 6×10^9 vg/eye leads to durable aflibercept expression and effectively inhibits laser-induced CNV formation in NHPs.

Pharmacokinetics and biodistribution of NG101 in NHPs

To complement the therapeutic findings, a detailed biodistribution analysis of NG101 was conducted on serum, VH, and AH (Tables 2 and 3). Notably, no detectable NG101 vector was found in the serum, AH, and VH of the vehicle group. In the groups administered NG101 at a dose of 3×10^9 vg/eye, vector levels remained below the limit of quantification (LOQ) at all evaluated time points in serum, except for two animals on day 3. At the higher dose of 6×10^9 vg/eye, detectable vector levels were observed in the serum on day 3 for three animals, declining by day 56 (Table 2). VH exhibited the highest NG101 vector levels compared to serum and AH. In VH, NG101 was detected in both eyes of two animals administered NG101 at 3×10^9 vg/eye and in the right eye of two animals administered NG101 at 6×10^9 vg/eye on days 86/88 (Table 3). AH results remained below the limit of detection (LOD) in all groups, except for the right eye of one animal administered NG101 at 3×10^9 vg/eye, which had a result below the LOQ (Table 3). Taken together, these data suggest that a single SR injection of NG101 results in predominant distribution of the vector within the eye.

For immune response analysis, anti-AAV8 neutralizing antibodies (NAbs) were evaluated. Serum samples collected during the predose phase and on days 29, 56, and 85 (Table 4) showed that four animals administered NG101 at 3×10^9 vg/eye and three animals administered NG101 at 6×10^9 vg/eye tested positive for anti-AAV8 NAbs at the predose phase. Following SR injection of NG101, there was an increasing tendency of anti-AAV8 NAbs. However, preexisting or increased levels of anti-AAV8 NAbs did not impact aflibercept expression in ocular tissues (Figures 3D–3G). Furthermore, anti-aflibercept antibodies were not detected in serum at the predose phase on days 29, 56, and 85 in all groups, nor were they detected in VH on days 86/88 (data not shown).

Ocular safety of NG101 in NHPs

Ophthalmic safety was assessed using slit-lamp biomicroscopy following a single SR injection of NG101 (Figure 4). The vehicle group exhibited transient anterior and posterior ocular inflammatory responses, characterized by the presence of aqueous cells, aqueous flares, and vitreous cells. Similar transient dose-related ocular inflammatory responses were noted in the NG101 groups, which resolved by day 60 without further ocular inflammatory response observed up to day 365. The SR injection sites in eyes administered NG101 were flat by day 8, and the laser spots were flat on days 86/88, approximately 4 weeks after CNV induction (data not shown). Additionally, there was no evidence of retinal toxicity based on electroretinography (ERG), flash-visual evoked potential (VEP), and intraocular pressure measurements in all groups (data not shown). These comprehensive evaluations demonstrate that NG101 induces only a transient and mild ocular inflammatory response at the effective dose range tested, without adverse effects on retinal structure and function.

DISCUSSION

NG101, a non-replicating rAAV8 viral vector, is designed to express aflibercept under the control of a synthetic CAT311 promoter. This promoter has been shown to induce robust and sustained ocular transgene expression for at least 51 weeks in mice (Figure S1). Our results indicate that the CAT311 promoter offers superior robustness and durability compared to the CAG promoter, enhancing gene expression and extracellular secretion of aflibercept in the eye. This is facilitated by the use by NG101 of a codon-optimized aflibercept

Figure 3. SR administration of NG101 effectively suppresses CNV formation at low doses in NHPs

NG101 (3×10^9 or 6×10^9 vg/eye) or vehicle (formulation buffer) was administered via SR injection on day 1 in cynomolgus monkeys. Eylea (2 mg/eye) was injected IVT on day 57, immediately following CNV induction. (A) Overview of efficacy testing in NHP CNV model. (B) Representative FA images are shown. (C) The percentage of grade 4 CNV lesions was evaluated. Data are shown as mean ± SD. (D–G) Aflibercept expression levels in the retina (D), choroid-RPE (E), vitreous humor (VH) (F), and aqueous humor (AH) (G) were measured at day 86/88 by ELISA. Additionally, two animals (one male and one female) from vehicle group and NG101 (3×10^9 and 6×10^9 vg/eye) groups were followed up until day 365. Data are shown as mean ± SD. (C–G) Statistical analysis: two-way ANOVA (C) and one-way ANOVA (D–G). (C) $^{****}p < 0.0001$ versus vehicle on day 71 and $^{###}p < 0.001$ and $^{####}p < 0.0001$ versus vehicle on day 85. ns, not significant. (D–G) $^{*}p < 0.05$; $^{**}p < 0.01$; $^{***}p < 0.001$ versus vehicle on day 86/88; $^{\#}p < 0.05$, $^{\#\#}p < 0.01$, $^{\#\#\#}p < 0.001$ versus Eylea on day 86/88; $^{\&}p < 0.05$ versus vehicle on day 365..

Table 2. Biodistribution of NG101 in serum

			Vehicle		3×10^9 vg/eye		6×10^9 vg/eye	
Sample	Time point	Sex	Animal ID	Copies/μg	Animal ID	Copies/μg	Animal ID	Copies/μg
Serum	predose	M	P0001	<LOD	P0201	<LOD	P0301	<LOD
			P0002	<LOD	P0202	<LOD	P0302	<LOD
			P0003	<LOD	P0203	<LOD	P0303	<LOD
		F	P0401	<LOD	P0501	<LOD	P0601	<LOD
			P0402	<LOD	P0503	<LOD	P0602	<LOD
			P0403	<LOD	P0504	<LOD	P0603	<LOD
	day 3	M	P0001	<LOD	P0201	<LOQ	P0301	<LOQ
			P0002	<LOD	P0202	<LOD	P0302	<LOQ
			P0003	<LOD	P0203	<LOD	P0303	219.24
		F	P0401	<LOD	P0501	<LOQ	P0601	<LOQ
			P0402	<LOD	P0503	473.64	P0602	908.96
			P0403	<LOD	P0504	847.99	P0603	199.01
	day 8	M	P0001	<LOD	P0201	<LOD	P0301	<LOQ
			P0002	<LOD	P0202	<LOD	P0302	<LOQ
			P0003	<LOD	P0203	<LOD	P0303	<LOQ
		F	P0401	<LOD	P0501	<LOD	P0601	<LOD
			P0402	<LOD	P0503	<LOQ	P0602	188.50
			P0403	<LOD	P0504	<LOQ	P0603	268.26
	day 29	M	P0001	<LOD	P0201	<LOD	P0301	<LOD
			P0002	<LOD	P0202	<LOD	P0302	<LOD
			P0003	<LOD	P0203	<LOD	P0303	<LOD
		F	P0401	<LOD	P0501	<LOD	P0601	<LOD
			P0402	<LOD	P0503	<LOQ	P0602	<LOD
			P0403	<LOD	P0504	<LOQ	P0603	<LOQ
	day 56	M	P0001	<LOD	P0201	<LOD	P0301	<LOD
			P0002	<LOD	P0202	<LOD	P0302	<LOD
			P0003	<LOD	P0203	<LOD	P0303	<LOD
		F	P0401	<LOD	P0501	<LOD	P0601	<LOD
			P0402	<LOD	P0503	<LOD	P0602	<LOD
			P0403	<LOD	P0504	<LOQ	P0603	<LOD

LOD, limit of detection; LOQ, limit of quantification.

gene along with a human IgG4 signal peptide sequence and a mutated WPRE sequence (Figures 1, 2, 3, and S2).[28,36] Additionally, the NG101 genome contains four copies of the target sequence for antigen-presenting cell (APC)-specific microRNA 142-3p.[29] This sequence serves to reduce aflibercept expression in APCs by promoting miR142-3p binding-mediated degradation of the mRNA, thereby decreasing the host immune response against aflibercept. Collectively, these elements contribute to robust and long-lasting aflibercept expression driven by NG101 in the retina, enhancing its therapeutic potential.

Various animal models of CNV, such as mice, rats, and NHPs, are used to evaluate treatment strategies for wAMD. In these models, a laser-induced rupture of Bruch's membrane results in the development of CNV.[37] Due to differences in eye size, typically, four CNV lesions are induced in the mouse eye, while nine lesions are created in NHP models. To evaluate the efficacy of NG101, we used both mouse and NHP laser-induced CNV models, with evaluation methods adapted to the anatomical differences. In the mouse model, vessel leakage is assessed by measuring fluorescence intensity in FA images of the entire eye, along with CNV volume based on OCT images (Figures 2C and 2E). In contrast, the NHP model allows for individual grading of CNV lesions based on the extent of leakage, with lesions classified from grades 1 to 4, where grade 4 represents clinically relevant leakage (Figure 3B).[35] A reduction in the occurrence of grade 4 lesions was used as an efficacy indicator. The close approximation of

Table 3. Biodistribution of NG101 in VH and AH

			Vehicle		3×10^9 vg/eye		6×10^9 vg/eye	
Sample	Time point	Sex	Animal ID	Copies/mL	Animal ID	Copies/mL	Animal ID	Copies/mL
VH-OD	day 86/88	M	P0001	<LOD	P0201	687,536.39	P0301	115,865.68
			P0002	<LOD	P0202	<LOQ	P0302	<LOQ
		F	P0401	<LOD	P0501	13,555,608.05	P0601	297143.72
			P0402	<LOD	P0503	<LOQ	P0602	<LOQ
VH-OS		M	P0001	<LOD	P0201	73,389.28	P0301	<LOQ
			P0002	<LOD	P0202	<LOQ	P0302	<LOQ
		F	P0401	<LOD	P0501	99,594.49	P0601	<LOQ
			P0402	<LOD	P0503	<LOQ	P0602	<LOQ
AH-OD	day 86/88	M	P0001	<LOD	P0201	<LOD	P0301	<LOD
			P0002	<LOD	P0202	<LOD	P0302	<LOD
		F	P0401	<LOD	P0501	<LOQ	P0601	<LOD
			P0402	<LOD	P0503	<LOD	P0602	<LOD
AH-OS		M	P0001	<LOD	P0201	<LOD	P0301	<LOD
			P0002	<LOD	P0202	<LOD	P0302	<LOD
		F	P0401	<LOD	P0501	<LOD	P0601	<LOD
			P0402	<LOD	P0503	<LOD	P0602	<LOD

AH, aqueous humor; LOD, limit of detection; LOQ, limit of quantification; OD, oculus dexter; OS, oculus sinister; VH, vitreous humor.

the NHP retina and macula to those of the human makes this grading system highly relevant.[37] Differences between mice and NHPs may account for variations in the efficacy of NG101 compared to Eylea (Figures 2 and 3). Alternatively, these differences may be due to the variable efficacy of Eylea at the given dose in each animal model. In the mice efficacy study, Eylea (40 μg/eye) showed incomplete suppression of blood vessel leakage, possibly due to insufficient aflibercept levels, whereas NG101, with its higher levels of aflibercept production, was able to provide better suppression. However, in the NHP efficacy study, the aflibercept levels in the Eylea group (2 mg/eye) were sufficient to nearly eliminate grade 4 lesions, resulting in comparable efficacy between NG101 and Eylea, despite the higher aflibercept expression of NG101. Overall, NG101 effectively suppressed CNV in both models, suggesting that in patients, it could offer efficacy comparable to Eylea while potentially reducing treatment burden through robust and long-lasting aflibercept expression.

Given that AAV is less pathogenic and the eye is an immune-privileged site, AAV ocular gene therapy is generally considered safe. However, high doses in many clinical trials have led to adverse effects such as ocular inflammation or retinal degeneration, particularly at doses above 1×10^{11} vg/eye. At doses ranging from 1×10^{10} to 1×10^{11} vg/eye, the occurrence of ocular inflammation has varied, with administration routes being more common with IVT injection compared to SR injection.[17] The most effective way to reduce the toxicity of the AAV vector is to lower its dose. Therefore, developing a strategy that enables the transgene to be expressed at an efficacious level with a minimal dose is crucial for patient safety.

NG101 has demonstrated effective inhibition of CNV at relatively low doses, specifically, 1×10^6 vg/eye in the mouse and 3×10^9 vg/eye in the NHP CNV models, owing to several key factors. First, the higher affinity of aflibercept for VEGF and its longer retinal residence time, compared to ranibizumab, enable effective VEGF inhibition with smaller amounts of therapeutic protein.[27,38] Second, the potent CAT311 promoter drives significantly higher expression levels of aflibercept at equivalent doses compared to the CAG promoter, facilitating a further reduction in the required vector dose (Figure S1). Lastly, SR injection targets NG101 delivery directly to the retina and RPE at the lesion site, optimizing local efficacy and minimizing systemic exposure (Figures 3D–3G and S2). The synergy between the high affinity of aflibercept for VEGF, the efficacy of the CAT311 promoter, and precise SR delivery enables NG101 to effectively curb CNV progression at these low doses.

Following NG101 administration, NG101 vectors were initially detected in serum on days 3 and 8, but levels quickly decreased to below the LOQ by day 56 in all subjects (Table 2). In ocular fluids, NG101 vectors were identified in the VH but not in the AH (Table 3). Additionally, anti-aflibercept antibodies were not detected in either the serum or VH, indicating no significant immunogenicity (data not shown). These observations confirm that the NG101 vector remains confined within the ocular environment after SR administration.

Despite the presence of anti-AAV NAbs (Table 4), which are known to potentially affect transduction efficiency and reduce efficacy following gene transfer,[39] ocular aflibercept expression remained

Table 4. Anti-AAV8 neutralizing antibody in serum

Group	Sex	Animal ID	Predose	Day 29	Day 56	Day 85
Vehicle	M	P0001	20	10	10	10
		P0002	<5	<5	<5	<5
		P0003	10	10	10	10
	F	P0401	5	<5	5	5
		P0402	<5	<5	<5	<5
		P0403	<5	5	<5	<5
Eylea, 2 mg/eye	M	P0101	320	–	–	–
		P0102	10	–	–	–
		P0103	160	–	–	–
3×10^9 vg/eye	M	P0201	80	20	80	40
		P0202	20	40	80	40
		P0203	80	80	80	80
	F	P0501	80	320	320	160
		P0503	<5	<5	<5	<5
		P0504	<5	<5	<5	<5
6×10^9 vg/eye	M	P0301	40	80	80	20
		P0302	10	80	40	40
		P0303	5	40	40	40
	F	P0601	40	1,280	320	160
		P0602	<5	5	<5	<5
		P0603	<5	5	20	10

Values are the reciprocal serum dilution at which relative luminescence units (RLUs) were reduced 50% compared to vector-only control wells.

unaffected in NHPs (Figures 3D–3G). This phenomenon underscores previous findings that such antibodies do not significantly inhibit transgene expression within ocular tissues, attributable to the protective nature of the blood-retinal barrier (BRB), which limits antibody penetration.[10,40,41] Furthermore, a previous study has shown that NAb levels are significantly lower in the VH than in serum across various serotypes in humans.[42] These findings suggest that the impact of preexisting anti-AAV NAbs on transgene expression in ocular tissues is likely less pronounced than in other tissues.

The ocular safety profile of NG101 was characterized by mild and transient inflammation, evident from aqueous cells, aqueous flare, and vitreous cells (Figure 4). This inflammation, which peaked 5 days post-injection in a dose-dependent manner, was also noted in the vehicle group, indicating that some responses could be attributed to the mechanical stimulation of the injection process. Importantly, this inflammation resolved completely by approximately 60 days post-injection, with no further inflammatory responses noted up to day 365. Retinal function, assessed by ERG and VEP tests, remained unaffected, indicating that these transient inflammatory responses did not compromise retinal function (data not shown).

In summary, a single SR administration of NG101 in mice and NHPs effectively suppresses CNV formation at low doses, ensuring robust and sustained expression of aflibercept within ocular tissues, particularly the retina. The NG101 treatment demonstrates a confined distribution within the eye, mild and transient ocular inflammation, and no retinal abnormalities, indicating its potential as a candidate for long-term treatment of wAMD. Based on these promising preclinical results, a phase 1/2a clinical trial for NG101 has been initiated to evaluate its safety and preliminary therapeutic efficacy in wAMD patients (this study is registered at ClinicalTrials.gov: NCT05984927). This trial uses significantly lower doses, ranging from 1×10^9 to 8×10^9 vg/eye, compared to other trials that have used doses ranging from 3×10^9 to 6×10^{11} vg/eye.[34,43,44]

MATERIAL AND METHODS

NG101 vector construction

NG101 is an rAAV8 vector containing a codon-optimized aflibercept gene, flanked by two ITR sequences. The NG101 vector genome is constructed using the Gibson Assembly method. Expression of aflibercept is controlled by a synthetic CAT311 promoter. The aflibercept gene is followed by multiple *cis*-elements, including the mWPRE, four copies of a target sequence for microRNA 142-3p (miR142-3pTx4), and the bGH pA.

SYPRO Ruby staining

Purified AAV samples were mixed with 4X Bolt LDS sample buffer (Invitrogen, Thermo Fisher Scientific, Waltham, MA). Following incubation at 95°C for 10 min, samples were loaded on a Bolt 4%–12% Bis-Tris plus gel (Invitrogen). Then, the gel was stained with SYPRO Ruby protein gel stain (Invitrogen) according to the manufacturer's instructions. Signals were detected using an automated imaging system (ChemiDoc; Bio-Rad Laboratories, Hercules, CA).

Immunoblot analysis

CHO-K1 cells were cultured in F-12K medium (American Type Culture Collection, , Manassas, VA) in a humidified atmosphere of 5% CO_2 at 37°C. Following pre-incubation with 5 μM MG132 (Sigma-Aldrich, St. Louis, MO) for 8 h, the cells were transduced with NG101 for 72 h, and the culture medium was collected. Eylea (aflibercept; Bayer AG, Leverkusen, Germany) and the samples were mixed with 4X Bolt LDS sample buffer (Novex). Proteins were separated by SDS-PAGE and transferred to a nitrocellulose membrane. The membrane was blocked with Tris-buffered saline containing 0.1% Tween 20 and 5% skim milk powder and then incubated with anti-human IgG antibody (709-035-149; The Jackson Laboratory, Bar Harbor, ME). Proteins were visualized using an enhanced chemiluminescence reagent (Thermo Fisher Scientific), and signals were detected using an automated imaging system (ChemiDoc; Bio-Rad Laboratories).

Aflibercept ELISA

HEK293 cells were cultured in DMEM containing 10% fetal bovine serum (Gibco, Thermo Fisher Scientific) in a humidified atmosphere of 5% CO_2 at 37°C. The cells were seeded and incubated for 18 h. Subsequently, the cells were pre-incubated with 5 μM of MG132 (Sigma-Aldrich) for 8 h. Then, the cells were transduced with NG101. After

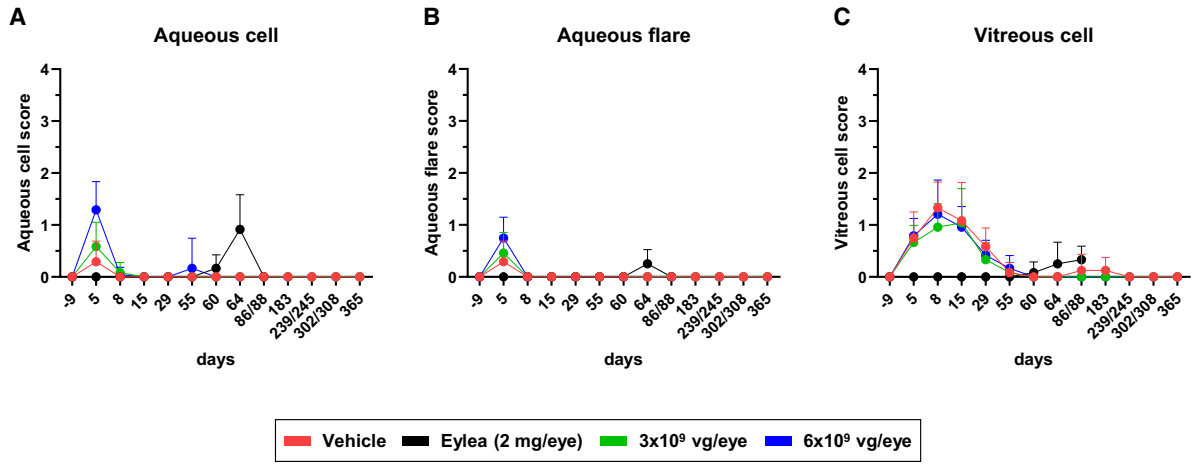

Figure 4. Ocular inflammation was mild and transient at the effective doses of NG101 in NHPs

Ophthalmic examinations were conducted on the same animals described in Figure 3 to assess ocular inflammatory responses. Parameters evaluated included aqueous cell (A), aqueous flare (B), and vitreous cells (C), monitored up to day 86/88. Additionally, two animals (one male and one female) from each of the vehicle and NG101 (3×10^9 and 6×10^9 vg/eye) groups were followed up until day 365. Data are shown as mean ± SD.

48 h, the culture medium was collected, and the aflibercept level was measured using an aflibercept ELISA kit (ImmunoGuide-AybayTech Biotechnology, Ankara, Türkiye) according to the manufacturer's instructions.

VEGF bioassay

VEGF bioassay (Promega, Fitchburg, WI) was performed according to the manufacturer's instructions. In brief, the collected cell culture medium containing NG101-derived aflibercept and Eylea (aflibercept; Bayer AG) were serially diluted using assay buffer. KDR/NFAT-RE HEK293 cells were resuspended in the assay buffer and dispensed into a 96-well assay plate. Then, diluted samples or Eylea was added, followed by the addition of VEGF-A_{165}. The assay plate was incubated at 37°C with 5% CO_2 for 6 h. Luminescence was measured using a Varioskan LUX multimode microplate reader (Thermo Fisher Scientific).

Ligand binding assay

The recombinant human (rh)VEGF-A_{165} (R&D Systems, Minneapolis, MN), rhPlGF (R&D Systems), and rhHGF (R&D Systems) were dispensed to a 96-well ELISA plate (Thermo Fisher Scientific) and incubated for 18 h. Then, 3% BSA and 0.05% Tween 20 in Dulbecco's PBS (DPBS; Gibco) was added and incubated for 1 h. Diluted samples or Eylea was added and incubated for 1 h, followed by washing with 0.1% Tween 20 in DPBS. Horseradish peroxidase-conjugated anti-human Fc IgG antibody (Invitrogen) was added and incubated for 1 h. Following washing with 0.1% Tween 20 in DPBS, TMB (Thermo Fisher Scientific) was added and incubated for 5 min for rhVEGF-A_{165} or 10 min for rhPlGF and rhHGF. Then, 1 N sulfuric acid (Samchun, Seoul, Korea) was added to stop the reaction. Absorbance was measured at 450 nm using a Varioskan Lux (Thermo Fisher Scientific).

Animal study approval

The mice studies were reviewed and approved by the Institutional Animal Care and Use Committees (IACUC) of KPC Co., Ltd. In accordance with the Animal Protection Act (Approval No.: P215004). All procedures for NHP studies were in compliance with applicable animal welfare acts and were approved by the local Institutional Animal Care and Use Committee (IACUC).

Dose administration

Mice

NG101 or vehicle (formulation buffer) was SR administered into both eyes (1 μL/eye) 28 days before CNV induction in C57BL/6 mice. A 31G needle was used to create a scleral puncture, through which a 34G needle connected to an IO kit (Nanofil-IO kit; World Precision Instruments, Sarasota, FL) was inserted. Subsequently, FP and OCT were used to check for bleb formation on the retina. Eylea was IVT administered into both eyes at (1 μL/eye) immediately after CNV induction. Following administration, an antibiotic eye drop formulation (Tobrex, Novartis Korea, Seoul, Korea) was applied once to each eye to prevent infections.

Cynomolgus monkeys

Cynomolgus monkeys were anesthetized with ketamine and dexmedetomidine. The eyes were cleaned with 1% povidone iodine solution. A 2.5% povidone iodine solution was used at the dose site prior to injection. Pupils were dilated with a topical mydriatic agent. A DORC 23G needle with an extendible 41G SR injection needle (DORC, Zuidland, the Netherlands) was introduced through the sclera in the superior temporal quadrant of the globe, approximately 3 mm posterior to the corneal limbus. The 41G cannula tip was advanced from the needle and gently touched to the retinal surface. NG101 or vehicle was injected through the neural retina into the SR space, resulting in a SR bleb. After the

injection, a topical antibiotic and steroid ointment (Neo-Poly-Dex) was instilled in each eye.

For IVT injection of Eylea, a topical anesthetic (0.5% proparacaine) was instilled in each eye before the procedure. A wire speculum was used to retract the eyelids. The eyes were cleaned with 1% povidone iodine solution and rinsed with sterile saline. A 30G needle was used for each dose. Following dosing, a topical antibiotic (Neo-Poly-Bac) was applied to each eye.

FP

For retinal imaging evaluation, mice were anesthetized with ketamine (Yuhan, Seoul, Korea) and xylazine (Bayer Korea, Seoul, Korea), and an anesthetic eye drop (Alcaine; Alcon Korea, Seoul, Korea) was applied to each eye for additional local anesthesia. Mydriasis was induced with mydriatics (Tropherine Eye Drops; Alcon Korea). The images were taken with a Micron IV (Phoenix-Micron, Bend, OR). After imaging was completed, a droplet of antibiotic eye drops (Tobrex 0.3% Eye Drops; Novartis Korea) was applied to each eye.

Image analysis for FP was performed using ImageJ, and the following formula was used to calculate the CTF:

Cynomolgus monkeys

Animals were anesthetized with ketamine and dexmedetomidine. The macula of each cynomolgus monkey's eye underwent laser treatment with a 532-nm diode green laser burns (OcuLight GL; Iridex, Mountain View, CA) using a slit-lamp delivery system, a single mirror lens (Ocular Instruments, Bellevue, WA), and plano fundus contact lens. The laser parameters included a spot size of 75 μm, duration of 0.1 s, and power of 400–650 mW. Nine areas were symmetrically placed in the macula of each eye.

FA/OCT

Mice

After inducing general anesthesia using xylazine and ketamine, mice received an intraperitoneal injection of 100 mg/kg fluorescent contrast agents (10% Fluorescite; Alcon Korea). The imaging camera of the Micron-IV system was focused on the fundus, and a hypromellose lubricant (Hycell Oph Soln; Samil Pharmaceutical, Seoul, Korea) was applied to the eye. The lens of the OCT system (Phoenix-Micron) was placed in contact with the cornea. Imaging was completed within 5 min. ImageJ was used to analyze FA and OCT images, and the CTF was calculated using Equation 1.

$$\text{Corrected total fluorescence (CTF)} = \text{Integrated Density} - (\text{Area of selected cell} \times \text{Mean fluorescence of background readings}) \quad \text{(Equation 1)}$$

GFP ELISA

The eyes were lysed using a TissueLyser (Qiagen, Hilden, Germany) with stainless steel beads (Qiagen) and radioimmunoprecipitation assay buffer (Thermo Fisher Scientific) containing a protease inhibitor (Thermo Fisher Scientific). The lysate was incubated for 1 h at 4°C and then centrifuged at 13,000 × *g* for 15 min. The supernatant was collected for analysis using a GFP ELISA kit (Abcam, Cambridge, UK).

CNV induction

Mice

C57BL/6 mice were anesthetized by the intraperitoneal injection of 10 mg/kg xylazine (Rompun; Bayer Korea) and 100 mg/kg ketamine (ketamine; Yuhan). An anesthetic eye drop (Alcaine) was applied to each eye, followed by a mydriatics (Tropherine Eyedrops; Alcon Korea). The imaging camera of the Micron-IV system was focused on the fundus. The conditions for CNV induction were as follows: wavelength 532 nm, diameter 50 μm, duration 80 ms, and power level 240 mW. One drop of an antibiotic (Tobrex; Novartis Korea) was applied to the eye. Burn lesions that showed no bubbling during lesion induction were classified as unsuccessful laser burns and were excluded from analyses according to the modified version of the exclusion criteria.[45]

Cynomolgus monkeys

Cynomolgus monkeys were anesthetized with ketamine and maintained on sevoflurane. Pupils were dilated with a mydriatic agent. Fluorescein was administered intravenously, and photographs were taken at the beginning and end of the injection. Stereophotographs of the right eye's posterior pole were taken rapidly from the dye appearance through 50 s, followed by stereopairs of the posterior pole at approximately at 1–2 and 5 min later. Between 2 and 5 min later, nonstereoscopic photographs of two mid-peripheral fields (temporal and nasal) in each eye were taken. For OCT, cynomolgus monkeys were anesthetized with ketamine, maintained on sevoflurane, and pupils were dilated with a mydriatic agent. A Spectralis HRA+ OCT instrument (Heidelberg Engineering, Franklin, MA) was used.

Ophthalmic examination

Cynomolgus monkeys were anesthetized with ketamine, and pupils were dilated with a mydriatic agent (1% tropicamide) prior to examination. The adnexa and anterior portion of both eyes were examined using a slit lamp biomicroscope. The ocular fundus of both eyes was examined using an indirect ophthalmoscope.

Biodistribution

DNA was extracted from blood and VH using the QIASymphony DSP DNA kit (Qiagen) and from AH using QIASymphony DSP

Virus/Pathogen Mini kit (Qiagen). To detect the transgene, qPCR was performed using 2× Environmental Master Mix (Applied Biosystems, Carlsbad, CA) in the QuantStudio Flex Real-Time PCR System (Applied Biosystems).

Anti-AAV8 NAb analysis

HEK293 cells were seeded into 96-well flat-bottom plates and incubated in a humidified atmosphere of 5% CO_2 at 37°C. On the following day, serum samples, previously heat treated at 56°C for 35 min, were serially diluted in medium starting at 1:5. The diluted samples or controls were then incubated with AAV8.CMV. LacZ.bGH vector (MOI of 1×10^4) for 1 h at 37°C. Subsequently, the incubated mixtures were transferred to the cells and incubated for 20–24 h in a humidified atmosphere of 5% CO_2 at 37°C. The transduced cells were lysed, developed using a chemiluminescent substrate, and read on a spectrophotometer.

Statistical analysis

GraphPad Prism 10 software was used to generate graphs and analyze data.

DATA AND CODE AVAILABILITY

The data supporting the findings of this study are available within the article and its supplemental information. In addition, it can be provided by contacting the corresponding author upon reasonable request.

ACKNOWLEDGMENTS

This study was primarily funded by Neuracle Genetics Inc. Reyon Pharmaceutical Co. Ltd. provided financial support for NG101 production. We appreciate NDIC and LabCorp for valuable technical support.

AUTHOR CONTRIBUTIONS

J.S. and J.B. conceived and designed the studies, with J.S. and J.S.H. providing supervision. J.B., S.S., and K.L. performed the *in vitro* assays. H.Y.K. and J.S.H. designed the NG101 vector and helper plasmids, while S.S., K.L., and Y.H.H. constructed the NG101 vector and helper plasmids. Y.K. wrote the original manuscript, and J.S., Y.K., J.B., and J.S.H. reviewed and edited the manuscript.

DECLARATION OF INTERESTS

H.Y.K., S.S., K.L., and J.S.H. have filed a patent application for CAT311 promoter (PCT/KR2021/008693). All authors are employees of Neuracle Genetics. Additionally, all authors, except Y.K., hold shares in Neuracle Genetics.

SUPPLEMENTAL INFORMATION

Supplemental information can be found online at https://doi.org/10.1016/j.omtm.2024.101366.

REFERENCES

1. Fleckenstein, M., Keenan, T.D.L., Guymer, R.H., Chakravarthy, U., Schmitz-Valckenberg, S., Klaver, C.C., Wong, W.T., and Chew, E.Y. (2021). Age-related macular degeneration. Nat. Rev. Dis. Primers *7*, 31. https://doi.org/10.1038/s41572-021-00265-2.

2. Liu, Y., Fortmann, S.D., Shen, J., Wielechowski, E., Tretiakova, A., Yoo, S., Kozarsky, K., Wang, J., Wilson, J.M., and Campochiaro, P.A. (2018). AAV8-antiVEGFfab Ocular Gene Transfer for Neovascular Age-Related Macular Degeneration. Mol. Ther. *26*, 542–549. https://doi.org/10.1016/j.ymthe.2017.12.002.

3. Pugazhendhi, A., Hubbell, M., Jairam, P., and Ambati, B. (2021). Neovascular Macular Degeneration: A Review of Etiology, Risk Factors, and Recent Advances in Research and Therapy. Int. J. Mol. Sci. *22*, 1170. https://doi.org/10.3390/ijms22031170.

4. Kovach, J.L., Schwartz, S.G., Flynn, H.W., Jr., and Scott, I.U. (2012). Anti-VEGF Treatment Strategies for Wet AMD. J. Ophthalmol. *2012*, 786870. https://doi.org/10.1155/2012/786870.

5. Kaiser, S.M., Arepalli, S., and Ehlers, J.P. (2021). Current and Future Anti-VEGF Agents for Neovascular Age-Related Macular Degeneration. J. Exp. Pharmacol. *13*, 905–912. https://doi.org/10.2147/JEP.S259298.

6. Nguyen, Q.D., Das, A., Do, D.V., Dugel, P.U., Gomes, A., Holz, F.G., Koh, A., Pan, C.K., Sepah, Y.J., Patel, N., et al. (2020). Brolucizumab: Evolution through Preclinical and Clinical Studies and the Implications for the Management of Neovascular Age-Related Macular Degeneration. Ophthalmology *127*, 963–976. https://doi.org/10.1016/j.ophtha.2019.12.031.

7. Grishanin, R., Vuillemenot, B., Sharma, P., Keravala, A., Greengard, J., Gelfman, C., Blumenkrantz, M., Lawrence, M., Hu, W., Kiss, S., and Gasmi, M. (2019). Preclinical Evaluation of ADVM-022, a Novel Gene Therapy Approach to Treating Wet Age-Related Macular Degeneration. Mol. Ther. *27*, 118–129. https://doi.org/10.1016/j.ymthe.2018.11.003.

8. Kiss, S., Oresic Bender, K., Grishanin, R.N., Hanna, K.M., Nieves, J.D., Sharma, P., Nguyen, A.T., Rosario, R.J., Greengard, J.S., Gelfman, C.M., and Gasmi, M. (2021). Long-Term Safety Evaluation of Continuous Intraocular Delivery of Aflibercept by the Intravitreal Gene Therapy Candidate ADVM-022 in Nonhuman Primates. Transl. Vis. Sci. Technol. *10*, 34. https://doi.org/10.1167/tvst.10.1.34.

9. Lai, C.M., Estcourt, M.J., Himbeck, R.P., Lee, S.Y., Yew-San Yeo, I., Luu, C., Loh, B.K., Lee, M.W., Barathi, A., Villano, J., et al. (2012). Preclinical safety evaluation of subretinal AAV2.sFlt-1 in non-human primates. Gene Ther. *19*, 999–1009. https://doi.org/10.1038/gt.2011.169.

10. Ke, X., Jiang, H., Li, Q., Luo, S., Qin, Y., Li, J., Xie, Q., and Zheng, Q. (2023). Preclinical evaluation of KH631, a novel rAAV8 gene therapy product for neovascular age-related macular degeneration. Mol. Ther. *31*, 3308–3321. https://doi.org/10.1016/j.ymthe.2023.09.019.

11. Wang, D., Tai, P.W.L., and Gao, G. (2019). Adeno-associated virus vector as a platform for gene therapy delivery. Nat. Rev. Drug Discov. *18*, 358–378. https://doi.org/10.1038/s41573-019-0012-9.

12. Naso, M.F., Tomkowicz, B., Perry, W.L., 3rd, and Strohl, W.R. (2017). Adeno-Associated Virus (AAV) as a Vector for Gene Therapy. BioDrugs *31*, 317–334. https://doi.org/10.1007/s40259-017-0234-5.

13. Yang, J., Zhou, W., Zhang, Y., Zidon, T., Ritchie, T., and Engelhardt, J.F. (1999). Concatamerization of adeno-associated virus circular genomes occurs through intermolecular recombination. J. Virol. *73*, 9468–9477. https://doi.org/10.1128/JVI.73.11.9468-9477.1999.

14. Penaud-Budloo, M., Le Guiner, C., Nowrouzi, A., Toromanoff, A., Chérel, Y., Chenuaud, P., Schmidt, M., von Kalle, C., Rolling, F., Moullier, P., and Snyder, R.O. (2008). Adeno-associated virus vector genomes persist as episomal chromatin in primate muscle. J. Virol. *82*, 7875–7885. https://doi.org/10.1128/JVI.00649-08.

15. Maurya, S., Sarangi, P., and Jayandharan, G.R. (2022). Safety of Adeno-associated virus-based vector-mediated gene therapy-impact of vector dose. Cancer Gene Ther. *29*, 1305–1306. https://doi.org/10.1038/s41417-021-00413-6.

16. Ertl, H.C.J. (2023). Mitigating Serious Adverse Events in Gene Therapy with AAV Vectors: Vector Dose and Immunosuppression. Drugs *83*, 287–298. https://doi.org/10.1007/s40265-023-01836-1.

17. Chan, Y.K., Wang, S.K., Chu, C.J., Copland, D.A., Letizia, A.J., Costa Verdera, H., Chiang, J.J., Sethi, M., Wang, M.K., Neidermyer, W.J., Jr., et al. (2021). Engineering adeno-associated viral vectors to evade innate immune and inflammatory responses. Sci. Transl. Med. *13*, eabd3438. https://doi.org/10.1126/scitranslmed.abd3438.

18. Hartman, R.R., and Kompella, U.B. (2018). Intravitreal, Subretinal, and Suprachoroidal Injections: Evolution of Microneedles for Drug Delivery. J. Ocul. Pharmacol. Ther. *34*, 141–153. https://doi.org/10.1089/jop.2017.0121.

19. Ail, D., Malki, H., Zin, E.A., and Dalkara, D. (2023). Adeno-Associated Virus (AAV) -Based Gene Therapies for Retinal Diseases: Where are We? Appl. Clin. Genet. *16*, 111–130. https://doi.org/10.2147/TACG.S383453.

20. Dalkara, D., Kolstad, K.D., Caporale, N., Visel, M., Klimczak, R.R., Schaffer, D.V., and Flannery, J.G. (2009). Inner limiting membrane barriers to AAV-mediated retinal

transduction from the vitreous. Mol. Ther. *17*, 2096–2102. https://doi.org/10.1038/mt.2009.181.

21. Dalkara, D., Byrne, L.C., Klimczak, R.R., Visel, M., Yin, L., Merigan, W.H., Flannery, J.G., and Schaffer, D.V. (2013). In vivo-directed evolution of a new adeno-associated virus for therapeutic outer retinal gene delivery from the vitreous. Sci. Transl. Med. *5*, 189ra76. https://doi.org/10.1126/scitranslmed.3005708.

22. Kotterman, M., Beliakoff, G., Croze, R., Vazin, T., Schmitt, C., Szymanski, P., Leong, M., Quezada, M., Holt, J., Barglow, K., et al. (2021). Directed Evolution of AAV Targeting Primate Retina by Intravitreal Injection Identifies R100, a Variant Demonstrating Robust Gene Delivery and Therapeutic Efficacy in Non-Human Primates. Preprint at bioRxiv. https://doi.org/10.1101/2021.06.24.449775.

23. Seitz, I.P., Michalakis, S., Wilhelm, B., Reichel, F.F., Ochakovski, G.A., Zrenner, E., Ueffing, M., Biel, M., Wissinger, B., Bartz-Schmidt, K.U., et al. (2017). Superior Retinal Gene Transfer and Biodistribution Profile of Subretinal Versus Intravitreal Delivery of AAV8 in Nonhuman Primates. Invest. Ophthalmol. Vis. Sci. *58*, 5792–5801. https://doi.org/10.1167/iovs.17-22473.

24. Holash, J., Davis, S., Papadopoulos, N., Croll, S.D., Ho, L., Russell, M., Boland, P., Leidich, R., Hylton, D., Burova, E., et al. (2002). VEGF-Trap: a VEGF blocker with potent antitumor effects. Proc. Natl. Acad. Sci. USA *99*, 11393–11398. https://doi.org/10.1073/pnas.172398299.

25. Stewart, M.W. (2012). Aflibercept (VEGF Trap-eye): the newest anti-VEGF drug. Br. J. Ophthalmol. *96*, 1157–1158. https://doi.org/10.1136/bjophthalmol-2011-300654.

26. Trichonas, G., and Kaiser, P.K. (2013). Aflibercept for the treatment of age-related macular degeneration. Ophthalmol. Ther. *2*, 89–98. https://doi.org/10.1007/s40123-013-0015-2.

27. Papadopoulos, N., Martin, J., Ruan, Q., Rafique, A., Rosconi, M.P., Shi, E., Pyles, E.A., Yancopoulos, G.D., Stahl, N., and Wiegand, S.J. (2012). Binding and neutralization of vascular endothelial growth factor (VEGF) and related ligands by VEGF Trap, ranibizumab and bevacizumab. Angiogenesis *15*, 171–185. https://doi.org/10.1007/s10456-011-9249-6.

28. Wang, L., Wang, Z., Zhang, F., Zhu, R., Bi, J., Wu, J., Zhang, H., Wu, H., Kong, W., Yu, B., and Yu, X. (2016). Enhancing Transgene Expression from Recombinant AAV8 Vectors in Different Tissues Using Woodchuck Hepatitis Virus Post-Transcriptional Regulatory Element. Int. J. Med. Sci. *13*, 286–291. https://doi.org/10.7150/ijms.14152.

29. Majowicz, A., Maczuga, P., Kwikkers, K.L., van der Marel, S., van Logtenstein, R., Petry, H., van Deventer, S.J., Konstantinova, P., and Ferreira, V. (2013). Mir-142-3p target sequences reduce transgene-directed immunogenicity following intramuscular adeno-associated virus 1 vector-mediated gene delivery. J. Gene Med. *15*, 219–232. https://doi.org/10.1002/jgm.2712.

30. Worner, T.P., Bennett, A., Habka, S., Snijder, J., Friese, O., Powers, T., Agbandje-McKenna, M., and Heck, A.J.R. (2021). Adeno-associated virus capsid assembly is divergent and stochastic. Nat. Commun. *12*, 1642. https://doi.org/10.1038/s41467-021-21935-5.

31. Moreno, M.R., Tabitha, T.S., Nirmal, J., Radhakrishnan, K., Yee, C.H., Lim, S., Venkatraman, S., and Agrawal, R. (2016). Study of stability and biophysical characterization of ranibizumab and aflibercept. Eur. J. Pharm. Biopharm. *108*, 156–167. https://doi.org/10.1016/j.ejpb.2016.09.003.

32. Gelfman, C.M., Grishanin, R., Bender, K.O., Nguyen, A., Greengard, J., Sharma, P., Nieves, J., Kiss, S., and Gasmi, M. (2021). Comprehensive Preclinical Assessment of ADVM-022, an Intravitreal Anti-VEGF Gene Therapy for the Treatment of Neovascular AMD and Diabetic Macular Edema. J. Ocul. Pharmacol. Ther. *37*, 181–190. https://doi.org/10.1089/jop.2021.0001.

33. Kiss, S., Grishanin, R., Nguyen, A., Rosario, R., Greengard, J.S., Nieves, J., Gelfman, C.M., and Gasmi, M. (2020). Analysis of Aflibercept Expression in NHPs following Intravitreal Administration of ADVM-022, a Potential Gene Therapy for nAMD. Mol. Ther. Methods Clin. Dev. *18*, 345–353. https://doi.org/10.1016/j.omtm.2020.06.007.

34. Busbee, B., Boyer, D.S., Khanani, A.M., Wykoff, C.C., Pieramici, D.J., Regillo, C., Danzig, C.J., Joondeph, B.C., Major, J., Hoang, C., et al. (2021). Phase 1 Study of Intravitreal Gene Therapy with ADVM-022 for neovascular AMD (OPTIC Trial). Investigative Ophthalmology Vis. Sci. *62*, 352.

35. Nork, T.M., Dubielzig, R.R., Christian, B.J., Miller, P.E., Miller, J.M., Cao, J., Zimmer, E.P., and Wiegand, S.J. (2011). Prevention of experimental choroidal neovascularization and resolution of active lesions by VEGF trap in nonhuman primates. Arch. Ophthalmol. *129*, 1042–1052. https://doi.org/10.1001/archophthalmol.2011.210.

36. Haryadi, R., Ho, S., Kok, Y.J., Pu, H.X., Zheng, L., Pereira, N.A., Li, B., Bi, X., Goh, L.T., Yang, Y., and Song, Z. (2015). Optimization of heavy chain and light chain signal peptides for high level expression of therapeutic antibodies in CHO cells. PLoS One *10*, e0116878. https://doi.org/10.1371/journal.pone.0116878.

37. Grossniklaus, H.E., Kang, S.J., and Berglin, L. (2010). Animal models of choroidal and retinal neovascularization. Prog. Retin. Eye Res. *29*, 500–519. https://doi.org/10.1016/j.preteyeres.2010.05.003.

38. Avery, R.L., Castellarin, A.A., Steinle, N.C., Dhoot, D.S., Pieramici, D.J., See, R., Couvillion, S., Nasir, M.A., Rabena, M.D., Maia, M., et al. (2017). Systemic Pharmacokinetics and Pharmacodynamics of Intravitreal Aflibercept, Bevacizumab, and Ranibizumab. Retina *37*, 1847–1858. https://doi.org/10.1097/IAE.0000000000001493.

39. Fitzpatrick, Z., Leborgne, C., Barbon, E., Masat, E., Ronzitti, G., van Wittenberghe, L., Vignaud, A., Collaud, F., Charles, S., Simon Sola, M., et al. (2018). Influence of Pre-existing Anti-capsid Neutralizing and Binding Antibodies on AAV Vector Transduction. Mol. Ther. Methods Clin. Dev. *9*, 119–129. https://doi.org/10.1016/j.omtm.2018.02.003.

40. Krader, C.G. (2021). Novel Gene Therapy for Neovascular AMD Showing Efficacy, Safety. https://www.ophthalmologytimes.com/view/novel-gene-therapy-for-neovascular-amd-showing-efficacy-safety.

41. Whitehead, M., Osborne, A., Yu-Wai-Man, P., and Martin, K. (2021). Humoral immune responses to AAV gene therapy in the ocular compartment. Biol. Rev. Camb. Philos. Soc. *96*, 1616–1644. https://doi.org/10.1111/brv.12718.

42. Lee, S., Kang, I.K., Kim, J.H., Jung, B.K., Park, K., Chang, H., Lee, J.Y., and Lee, H. (2019). Relationship Between Neutralizing Antibodies Against Adeno-Associated Virus in the Vitreous and Serum: Effects on Retinal Gene Therapy. Transl. Vis. Sci. Technol. *8*, 14. https://doi.org/10.1167/tvst.8.2.14.

43. Campochiaro, P.A., Avery, R., Brown, D.M., Heier, J.S., Ho, A.C., Huddleston, S.M., Jaffe, G.J., Khanani, A.M., Pakola, S., Pieramici, D.J., et al. (2024). Gene therapy for neovascular age-related macular degeneration by subretinal delivery of RGX-314: a phase 1/2a dose-escalation study. Lancet *403*, 1563–1573. https://doi.org/10.1016/S0140-6736(24)00310-6.

44. Khanani, A.M., Hershberger, V.S., Kay, C.N., Hu, A., Eichenbaum, D.A., Jaffe, G.J., Chung, C., Honarmand, S., Nien, C., and Lee, S. (2023). Interim results for the Phase 1/2 PRISM Trial evaluating 4D-150, a dual-transgene intravitreal genetic medicine in individuals with neovascular (wet) age-related macular degeneration. Invest. Ophthalmol. Vis. Sci. *64*, 5055.

45. Gong, Y., Li, J., Sun, Y., Fu, Z., Liu, C.H., Evans, L., Tian, K., Saba, N., Fredrick, T., Morss, P., et al. (2015). Optimization of an Image-Guided Laser-Induced Choroidal Neovascularization Model in Mice. PLoS One *10*, e0132643. https://doi.org/10.1371/journal.pone.0132643.